Skeletal dimensions as predictors for the shape of the nose in a South African sample: a cone-beam computed tomography (CBCT) study

AF RIDEL[1], F DEMETER[12], J LIEBENBERG[1], EN L'ABBÉ[1], D VANDERMEULEN[1,3], AC OETTLÉ[1,4]

Alison Ridel (corresponding author)
[1]Department of Anatomy, Faculty of Health Sciences, University of Pretoria, Pretoria, South Africa.
E-mail : u16385676@tuks.co.za
E-mail : Alison.ridel.up@gmail.com
Tswelopele Building
University of Pretoria, Private Bag X323
Arcadia 0007, South Africa.

Fabrice Demeter
[2]Musée de l'Homme, UMR7206, 17 Place du Trocadéro, 75116 Paris, France.
[1]Department of Anatomy, Faculty of Health Sciences, University of Pretoria, Pretoria, South Africa.
E-mail : Fabrice.demeter@mnhn.fr

Jade Liebenberg
[1]Department of Anatomy, Faculty of Health Sciences, University of Pretoria, Pretoria, South Africa.
E-mail: u11031230@tuks.co.za
E-mail: jadel92@hotmail.com

Ericka N L'Abbe
[1]Department of Anatomy, Faculty of Health Sciences, University of Pretoria, Pretoria, South Africa.
E-mail : Ericka.Labbe@up.ac.za

Dirk Vandermeulen
[3]Center for Processing Speech and Images (PSI), Department of Electrical Engineering (ESAT), KU Leuven, Belgium.
[1]Department of Anatomy, Faculty of Health Sciences, University of Pretoria, Pretoria, South Africa.
E-mail: Dirk.vandermeulen@kuleuven.be

Anna C. Oettlé
[1]Department of Anatomy, Faculty of Health Sciences, University of Pretoria, Pretoria, South Africa.
[4]Department of Anatomy, School of Medicine, Sefako Makgatho Health Sciences University, Ga-Rankuwa, Pretoria, South Africa.
E-mail : Anna.oettle@smu.ac.za

Highlights

- South African groups had significantly different hard-and soft-tissue morphology.
- Predictors of the nose in black South Africans differed from white South Africans.
- Specific regression equations were developed for both South African groups.

Abstract

The profile of the nose is an important feature for facial approximations. Although several manual and semi-automated prediction guidelines exist for estimating the shape of the nose, the reliability and applicability of these methods to South Africans groups are unknown. The aim of this study was to predict the displacements of capulometric landmarks from hard-tissue planes to facilitate nasal soft-tissue reconstruction in a South African sample. Cone Beam Computed Tomography (CBCT) scans of 120 adult South Africans were selected from the Oral and Dental Hospital, University of Pretoria, South Africa. Measurements involving craniometric and capulometric landmarks of the nose were obtained as plane-to-plane distances. Correlation coefficients between hard- and soft-tissue measurements were determined, and regression equations computed to assist in the prediction of the most probable shape and size of the nose. All hard- and soft-tissue measurements appeared significantly different between groups, except for the distance between the pronasale and nasion in the transverse plane and for the distance between the alare and the nasion in the coronal plane. The nasal height, nasal bone length and the nasal bone projection were significant predictors of the pronasale, subnasale and alare positions. More precisely, the nasal height and the nasal bone length were significant predictors of the pronasale position in both groups. Nasal bone projection was only useful for predicting shape in white South Africans. The variation in the skeletal predictors of the external shape of the nose noted between black and white South Africans and the results of the cross-validation testing emphasize the need for population specific guidelines.

Keywords: human variability; facial approximation; regression equations; craniometric landmarks; capulometric landmarks; plane-to-plane distances.

Introduction

Facial features, especially the profile of the nose, are important in facial recognition and are of paramount consideration in forensic facial approximations [1-3]. Dimensions of the nose might be important in distinguishing male and female faces and are useful in establishing an accurate facial approximation of a missing person through craniofacial reconstruction [4]. Craniofacial reconstruction (CFR) focuses on the relationship between the external envelope of tissue and the internal skeletal substrate. As the nose is a complex component, with the underlying bone being only a minor substructure of the mid-facial cranium, the region needs to be analysed separately from the rest of the mid-face so as to assess the correlation between the skeletal substructures of the nose and its external surface morphology.

The morphology of the nose is often manually reconstructed from the shape and size of the nasal aperture, represented by the position of the pronasale, subnasale, and alare landmarks [5-9]. However, the reliability of this method depends on the characteristics of the sample population [9,10]. For example, the utilization of cadaver samples may be responsible for distortion of the soft-tissue data as desiccation appears within a few hours after death [11]. To overcome the limitations of tissue desiccation in cadavers, a variety of nose approximation methods in living populations have been developed based on the recent development in digital imaging techniques such as cephalograms [9,12] and computer tomography (CT) scans [13-15]. However, the utilization of CT scans as initial references may involve a supination effect on the face due to the horizontal position of the patient during scanning [16-17]. Moreover, the slice thickness, which generally ranges from 0.6 mm to 1.5 mm [13-15], may induce errors in the manual landmark placement on 3D surfaces.

More recently, cone-beam computed tomography (CBCT) scanning from living patients has been used. During a CBCT scan, the patient is seated in a vertical position while the X-ray source and detector rotate around the head, capturing images using a cone-shaped X-ray beam. The advantages of CBCT compared to CT include lower radiation dose, lower cost, and higher spatial resolution (0.1 mm to 0.4 mm) for the placement of 3D landmarks [18]. Using in vivo CBCT scanning does not only eliminate the effect of desiccation, but also possible supination effects.

Recently, Lee and collaborators [19] used CBCT scans to investigate the relationship between the external- and skeletal- dimensions of the nose so as to predict the nasal morphology of a Korean population. Measurements were obtained as point-to-plane distances or plane-to-plane distances by using well defined landmarks on the nasal skeleton and the external surface of the nose. This method estimates the coordinates of capulometric landmarks from the hard-tissue by predicting the distances of the capulometric landmarks from planes defined through craniometric landmarks. For example, the 3D position of the alare can be reconstructed from its distances from three mutually orthogonal planes (e.g. sagittal, coronal and transverse planes through the hard tissue nasion landmark). However, the reproducibility of the method described by Lee and collaborators [19] is unknown and has not yet been tested.

The aim of our study was to predict the relative positions of capulometric landmarks from hard-tissue planes to facilitate nasal soft-tissue reconstruction in a South African sample. Distances between landmarks (craniometric and capulometric) and planes were assessed. We examined the correlations among these measurements and established regression equations. We also assessed the reproducibility of all measures, which was not done by Lee and collaborators [19].

Materials & Methods

Cone Beam Computer Tomography (CBCT) scans of 120 adult South Africans were selected from the Oral and Dental Hospital, University of Pretoria, South Africa. CBCT scans were obtained using a CBCT scanner (Planmeca ProMax ® 3D) with the following properties: 90 kV, 11.2 mA, voxel size of 0.4 mm, and field of view of 230 x 260 mm. A total of 60 black (37 males and 23 females) and 60 white (32 males and 28 females) South Africans were selected (Table 1). In this study, the terms black and white South Africans were used as these social terms are required when describing a missing person. We selected young adults between 18 to 30 years old in order to exclude possible remodelling effect of the facial skeleton with the advancement of age. In order to obtain a standardized volume data set, the subjects were scanned in the seated position with their eyes closed and with a relaxed facial expression. Patients were excluded if they presented with any condition that could affect the morphology of the face (e.g. orthodontic treatment, pathological conditions, facial asymmetry or any facial interventional reconstructive surgery). This research project was approved by the Main Research Ethics Committee of the Faculty of Health Sciences, University of Pretoria, South Africa (Ethics Reference No: 301/2016).

Table 1. South African sample used.

Complete Sample		Black South African			White South African		
N	Age	Male	Female	Age	Male	Female	Mean Age
120	Mean: 27.15 (SD: 8.12)	37	23	Mean: 27.70 (SD: 7.18)	32	28	Mean: 26.25 (SD:9.1)

In order to obtain a standardized orientation of the planes, special care was taken in orienting all scans in the Frankfurt Horizontal (FH) plane using Fiji software [20]. The FH plane is defined by the right and left porion points (located at the top of each external acoustic meatus) and the left orbital (located at the bottom of the left orbit). Then, a reslicing process was performed on all DICOM images orienting all 3D head images in the same position. These resliced CBCT scans were imported into 3D Slicer software [21], version 4.8 for Windows for all measurements. Hard- and soft-tissue surface meshes were generated by finding the threshold values between segmented components according to the "Half Maximum Height" (HMH) quantitative iterative thresholding method [22]. Threshold values for hard-tissue varied between 1200-1250, and for the soft-tissue between 400-450. Sagittal, coronal and transverse planes corresponding to the resliced images were visualized and used as an instrument of measurement. In this study, the facial skeleton will be referred to as the hard-tissue, and the external structure of the nose as the soft-tissue.

Following the literature regarding facial approximation of the nose using CBCT scans [19] and in order to conserve homology and comparability between studies, craniometric and capulometric landmarks (type I, II, and III [23, 24]) selected in the study by Lee and collaborators [19] were used. Four craniometric landmarks (nasion (n), rhinion (rhi), nasospinale (ns) and alare (al)) were identified on the nasal bone and periphery of the nasal aperture, while three capulometric landmarks (pronasale (pn'), subnasale (sn') and alare (al')) were considered to represent the external structure of the nose. A total of seven landmarks described in Table 2 and illustrated in Fig. 1 were used.

Table 2. Definition and abbreviation of craniometric and capulometric landmarks used [23, 24].

	Landmarks	Abbreviation	Definition
Craniometric	Nasion	n	Intersection of the nasofrontal sutures in the median plane.
	Rhinion	rhi	Most rostral (end) point on the internasal suture.Cannot be determined accurately if nasal bones are broken distally.
	Nasospinale	ns	The point where a line drawn between the inferior most points of the nasal aperture crosses the median plane. Note that this point is not necessarily at the tip of the nasal spine.
	Alare	al	Instrumentally determined as the most lateral point on the nasal aperture in a transverse plane.
Capulometric	Pronasale	Pn'	The most anteriorly protruded point of the apex nasi. In the case of a bifid nose, the more protruding tip is chosen.
	Subnasale	Sn'	Median point at the junction between the lower border of the nasal septum and the philtrum area.
	Alare	Al'	The most lateral point on the nasal ala.

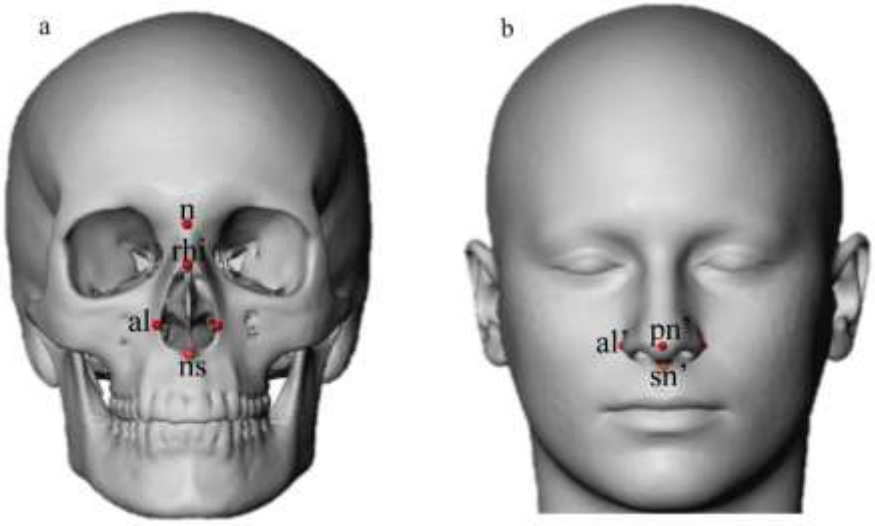

Figure 1. Landmarks placed on the hard- and soft-tissue.
n, nasion; rhi, rhinion; ns, nasospinale; al, alare; pn', pronasale; sn', subnasale; al', alare (cf. Table 2).

In order to assess the 3D external structure of the nose and related skeletal-tissue structures, a set of coronal, sagittal and transverse planes were defined through the identified landmarks. The planes on the hard-tissue included the nasion transverse plane (nTr), rhinion transverse plane (rhiTr), nasospinale transverse plane (nsTr), left alare sagittal plane (alLSa), right alare sagittal plane (alRSa), nasion coronal plane (nCor), rhinion coronal plane (rhiCor). A total of seven hard-tissue planes, described in Table 1 in supplementary material and illustrated in Fig. 2, were used.

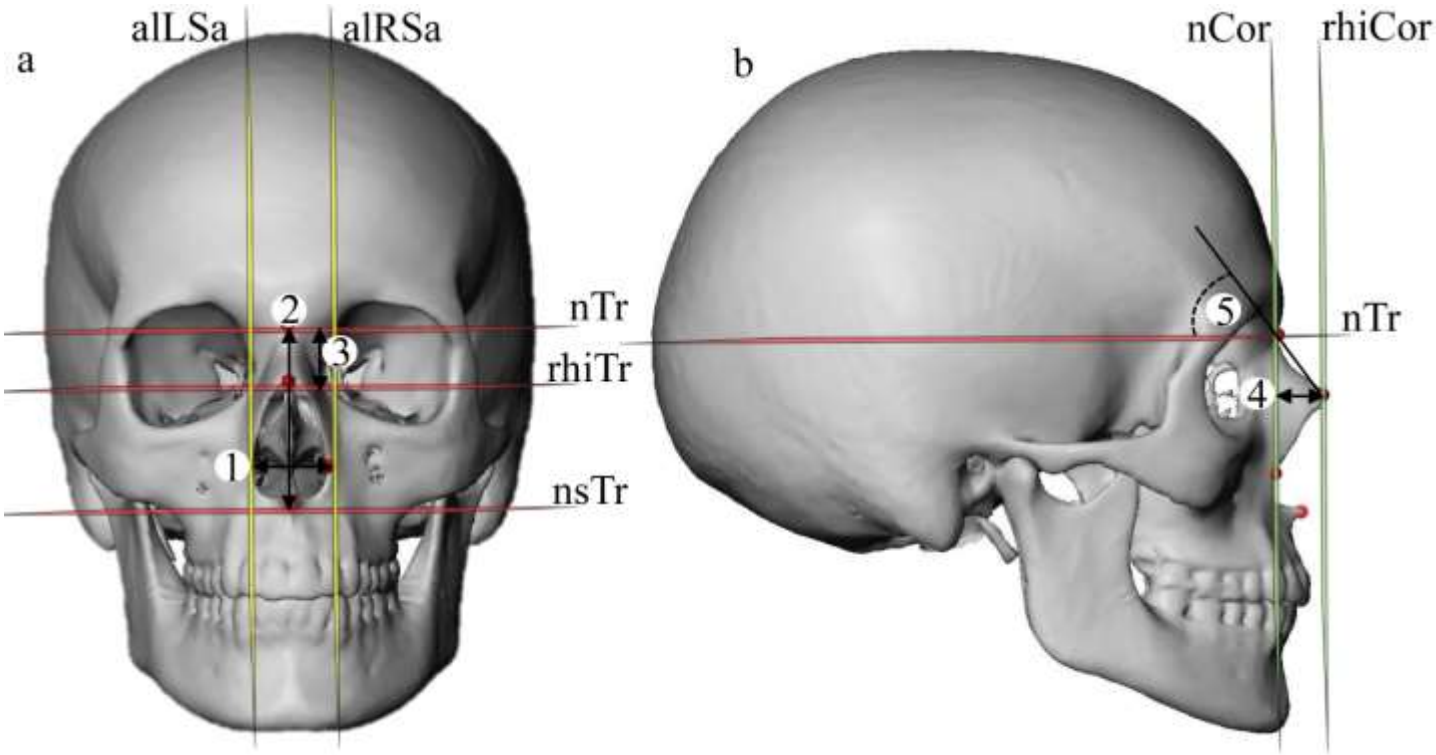

Figure 2. Hard-tissue transverse, sagittal and coronal planes and measurements.
a: Frontal view of the hard-tissue planes and measurements: nTr, nasion transverse plane; rhiTr, rhinion transverse plane; nsTr, nasospinale transverse plane; alSa, alare sagittal plane (left and right); 1, nasal width; 2, nasal height; 3, nasal bone length.
b: Lateral view of the hard-tissue planes and measurements: nCor, nasion coronal plane; rhiCor, rhinion coronal plane; 4, nasal bone projection; 5, nasal bone angle (cf. Table 1 in supplementary material).

The planes on the soft-tissue included the pronasale transverse plane (pn'Tr), left alare transverse plane (al'LTr), subnasale transverse plane (sn'Tr), subnasale coronal plane (sn'Cor), pronasale coronal plane (pn'Cor), left alare sagittal plane (al'LSa), right alare sagittal plane (al'RSa), left alare coronal plane (al'LCor). A total of eight soft-tissue planes, described in Table 1 in supplementary material and illustrated in Fig. 3, were used.

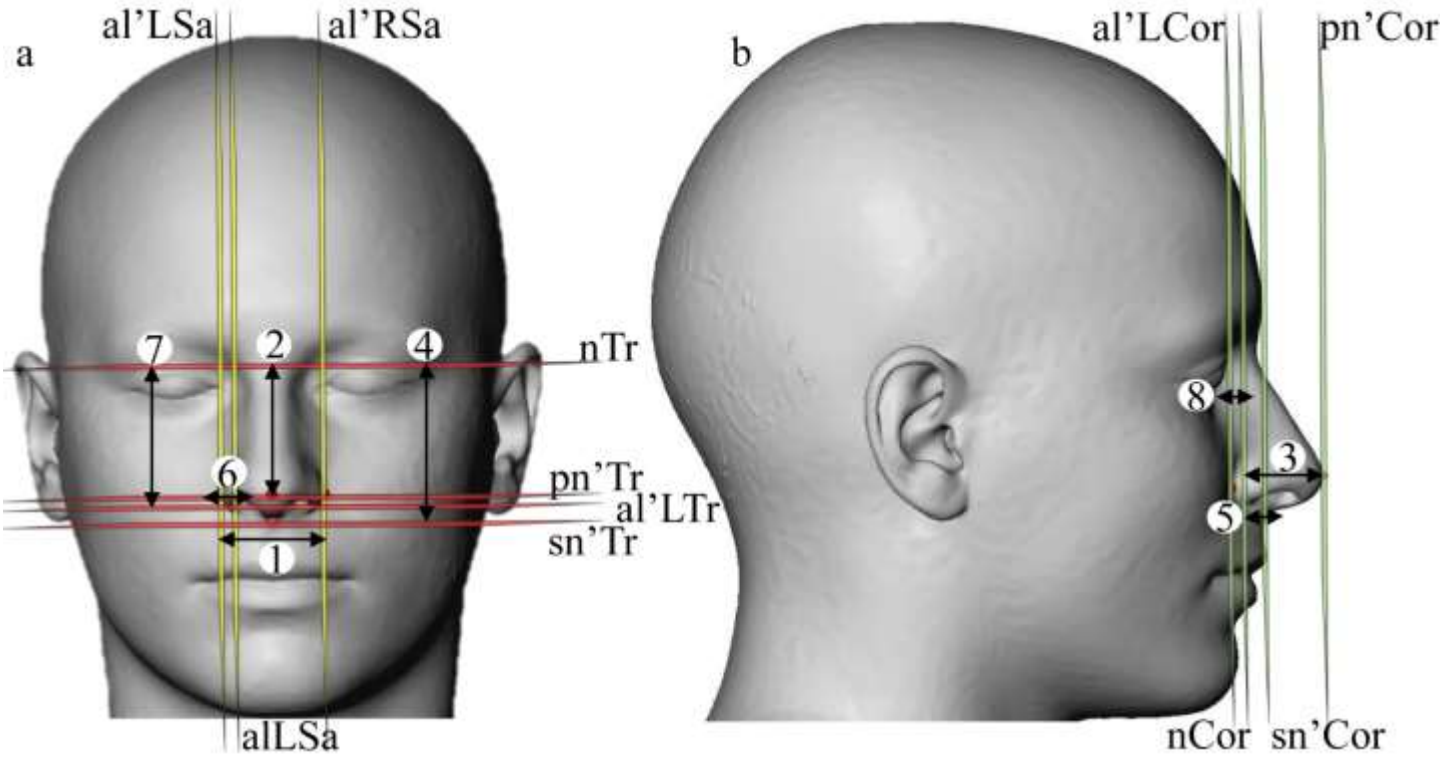

Figure 3. Soft-tissue transverse, sagittal and coronal planes and measurements.
a: Frontal view of the soft-tissue planes and measurements: nTr, nasion transverse plane; pn'Tr, pronasale transverse plane; al'Tr, alare transverse plane (left); sn'Tr, subnasale transverse plane; al'Sa, alare sagittal plane (left and right); 1, alare width; 2, pronasale to nasion transverse plane; 4, subnasale to nasion transverse plane; 6, alare to right nasal cavity sagittal plane; 7, alare to nasion transverse plane.
b: Lateral view of the soft-tissue planes and measurements: nCor, nasion coronal plane; sn'Cor, subnasale coronal plane; al'Cor, alare coronal plane (left); pn'Cor, pronasale coronal plane; 3, pronasale to nasion coronal plane; 5, subnasale to nasion coronal plane; 8, alare to nasion coronal plane (cf. Table 1 in supplementary material).

All measurements (M) were calculated as distances (in mm) between parallel planes. Thanks to the reslicing this reduces to taking absolute differences between the x, y or z coordinate value defining the plane.

The hard-tissue measurements included the nasal dimensions: nasal width, nasal height, nasal bone length, nasal bone projection and nasal bone angle. Only the nasal bone angle measurement was calculated using 3D hand tools. In order to represent the soft-tissue, measurements between the pn' and sn' planes (pn'Tr, pn'Cor, sn'Tr, sn'Cor) and each hard-tissue plane (nTr and nCor) were determined as well as between the al' planes (al'LSa, al'LTr and al'LCor) and each hard-tissue reference plane (alLSa, nTr, and nCor). The Alare width was measured by using the al'LSa and al'RSa planes. A total of 13 measurements described in Table 1 in supplementary material and illustrated in Figs. 2 and 3 were recorded.

Statistical analysis

In order to assess reproducibility and to have a quantification of errors induced, a test of the repeatability of the digitization in terms of inter- and intra-observer errors was performed. The method error (ME) of the double registration of all measurements was calculated using Dahlberg's [25] formula:

$$ME = \sqrt{\sum_{i=1}^{n} \frac{d_i^2}{2n}}$$

where *d* is the difference between two measurements and *n* is the number of subjects. For the inter-observer error, the images from 20 subjects (10 males and 10 females) were selected randomly and the measurements were performed twice by two different observers. For the intra-observer error, the images from 10 subjects (5 males and 5 females) were selected and the measurements were recorded twice with an interval of two weeks. According to the craniometric literature [26], an error will be considered acceptable in this study if the deviation is less than 2 mm. The Bland-Altman [27] plot was used to visually assess the degree of agreement between observers. In this method, the difference between the measurements is plotted against their mean. Additionally, lines corresponding to bias (defined as the mean (over all measurements) difference) and lower and upper limits of a 95%. Confidence Interval (CI) are plotted as well.

In order to assess the normality of the measurements, the Shapiro Wilk test was used. Means and standard deviations of measurements were computed in each South African group. An independent t-test was used to test for differences between sexes and ancestry. In order to determine whether the hard-tissue structure correlated to the soft-tissue of the nose, Pearson correlation analysis between measurements representing the position of the nose was applied. In addition, stepwise multiple regression analysis was used to determine whether skeletal-tissue measurements were able to predict the external surface measurements. The performance of equation regressions was assessed by estimating the Mean Squared Error (MSE) using leave-one-out cross-validation (LOOCV). The MSE is estimated from the training data and comparing it to the MSE of the predicted data (MSEP) [28]. Validation of the regression equations was also performed by using a 10-fold cross-validation process [29,30]. In each round, 90% of the subjects were used for training and 10% of the subjects are used for testing. The tests were repeated 10 times so that every subject had been tested once.

Significance was set at $p < 0.05$ for all tests. All statistical analyses were carried out with the R-studio software, version 1.0.44-®2009-2016 for Windows [31].

Results

According to the Shapiro Wilk test for multivariate normality, the sample is distributed normally (Shapiro Wilk test: p-value=0.2). Separate tests of univariate normality for each measurement were also performed (Table 1 in supplementary material). The inter- and intra-observer tests showed that all measurements were reproducible (Table 1 in supplementary material). Bland and Altman plots of the inter- and intra-observer errors are in Figs. 1 and 2 in supplementary material. These plots show that, apart from a limited number of outliers, the measurements for the inter- and intra-observations were located within the 95% CI, visually indicating a high degree of inter- and intra-observer agreement.

The means and standard deviations of the measurements involving pn', sn', and al' for the South African sample are given in Tables 3 and 4. All hard- and soft-tissue measurements were significantly different between black and white South Africans (see Table 3), except for the distance between the pronasale to the nasion transverse plane and the distance between the alare to the nasion coronal plane. On account of these differences black and white South Africans were analysed separately (Table 4). For black South Africans, males and females were significantly different for nasal height and distances: pn' to nTr, sn' to nTr, al' to alLSa and nTr, whereas white South Africans males and females were significantly different for the nasal width, nasal height, alare width, alare width/nasal width, and distances: pn' to nTr, sn' to nTr, al' to alLSa, al' to nTr and nCor.

Table 3. Means and standard deviations of the measurements in mm for the South African sample.

Measurements			Male		Female		Population difference
	Mean	SD	Mean	SD	Mean	SD	*P-value*
Nasal width	25.86	2.79	26.39	2.39	25.11	3.08	0.00
Nasal height	50.68	3.76	52.05	3.83	49.05	2.96	0.04
Nasal bone length	19.39	3.54	20.03	3.61	18.62	3.33	0.01
Nasal bone projection	10.25	4.13	9.43	4.08	11.21	4.02	0.00
Nasal bone angle (°)	66.7	7.69	68.55	7.15	64.52	7.79	0.00
Alare width	39.63	6.00	42.15	5.35	36.64	5.34	0.00
Alare width/Nasal width	153.72	18.23	160.09	18.29	146.25	15.37	0.00
Pronasale to Nasion Transverse plane	41.12	4.87	42.88	5.01	39.04	3.78	0.36
Pronasale to Nasion Coronal plane	28.90	7.21	28.04	7.90	29.91	6.22	0.00
Subnasale to Nasion Transverse plane	52.83	4.78	54.20	5.16	51.19	3.73	0.01
Subnasale to Nasion Coronal plane	14.87	7.18	13.40	7.51	16.60	6.40	0.00
Alare to Right Nasal Cavity Sagittal plane	6.76	2.39	7.63	2.42	5.73	1.92	0.00
Alare to Nasion Transverse plane	45.84	4.64	47.21	4.92	44.20	3.70	0.00
Alare to Nasion Coronal plane	6.60	3.84	5.81	3.25	7.52	4.34	0.34

Significant values ($p < 0.05$*) are indicated in bold.*

Table 4. Means and standard deviations of the measurements in mm for the black and white South African sample.

Measurements	Black South African					White South African				
	Male		Female		Sex difference	Male		Female		Sex difference
	Mean	SD	Mean	SD	*P-value*	Mean	SD	Mean	SD	*P-value*
Nasal width	27.34	2.28	27.83	1.94	0.37	25.13	1.95	23.17	2.13	0.00
Nasal height	51.28	3.32	47.91	2.32	0.00	53.07	4.27	49.87	3.14	0.00
Nasal bone length	20.69	3.51	19.38	2.62	0.10	19.16	3.61	18.08	3.71	0.25
Nasal bone projection	7.66	4.07	8.40	3.22	0.44	11.78	2.72	13.24	3.27	0.06
Nasal bone angle (°)	70.66	7.07	67.08	6.95	0.57	65.76	6.35	62.68	7.95	0.75
Alare width	45.78	3.52	42.06	2.95	0.33	37.34	3.06	32.74	2.47	0.00
Alare width/Nasal width	168.17	14.52	151.56	11.23	0.34	149.41	17.14	142.44	16.92	0.00
Pronasale to Nasion Transverse plane	42.47	4.84	37.89	3.63	0.00	43.42	5.27	39.87	3.72	0.00
Pronasale to Nasion Coronal plane	23.97	7.27	25.46	5.22	0.36	33.41	4.98	33.11	4.78	0.81
Subnasale to Nasion Transverse plane	53.19	5.06	49.51	3.30	0.00	55.54	5.06	52.40	3.59	0.00
Subnasale to Nasion Coronal plane	10.10	7.48	13.72	6.96	0.06	17.77	4.94	18.67	5.14	0.49
Alare to Right Nasal Cavity Sagittal plane	8.65	2.22	6.97	1.67	0.00	6.27	1.98	4.83	1.57	0.00
Alare to Nasion Transverse plane	46.12	4.72	42.30	3.58	0.00	48.65	4.88	45.57	3.19	0.00
Alare to Nasion Coronal plane	6.02	3.04	6.64	4.33	0.55	5.54	3.54	8.15	4.31	0.01

Significant values ($p < 0.05$*) are indicated in bold.*

Correlations of the hard- and soft-tissue dimensions with the capulometric landmarks: pn', sn', and al' in black South Africans are shown in Table 5 and white South Africans in Table 6. In both groups, the measurements of pn' to nTr, sn' to nTr, and al' to nTr, indicating the inferosuperior position of the pronasale, subnasale, and alare, respectively, showed significant correlations with the nasal height and nasal bone length. The measurement of sn' to nCor, highlighting the anteroposterior position of the subnasale, also showed a significant correlation with the nasal bone projection in both groups, while the measurement of pn' to nCor distinguishing the anteroposterior position of the pronasale showed a significant correlation with the nasal bone projection only in white South Africans. In addition, the measurement of pn' to nCor showed a significant correlation with the nasal bone length only in black South Africans. The measurements of the al' to alLSa and al' to nCor respectively indicating the inferosuperior and anteroposterior position of the Alare, did not show significant correlations with any skeletal measurements in both groups. Finally, the nasal width and the nasal bone angle did not correlate significantly with any surface measurements in both groups. All significant correlations were used in creating stepwise multiple regression equations for predicting the morphology of the nose of black and white South Africans.

Table 5. Correlation coefficient between hard-and soft-tissue measurements in mm of the black South African sample.

	Black South African				
Measurements	Nasal width.	Nasal height.	Nasal bone length.	Nasal bone projection.	Nasal bone angle
Pn' to nTr	0.08	**0.80**	-0.14	0.03	-0.24
Pn' to nCor	0.08	-0.05	**0.69**	0.15	0.16
Sn' to nTr	0.07	**0.80**	**0.73**	0.15	-0.24
Sn' to nCor	-0.01	-0.26	-0.24	**0.53**	0.26
Al' to alLSa	-0.30	0.02	-0.16	0.09	0.28
Al' to nTr	0.08	**0.74**	**0.65**	0.08	-0.16
Al' to nCor	-0.10	-0.21	-0.29	0.17	0.15

Significant correlations ($p < 0.05$*) are indicated in bold.*

Table 6. Correlation coefficient between hard-and soft-tissue measurements in mm of the white South African sample.

	White South African				
Measurements	Nasal width.	Nasal height.	Nasal bone length.	Nasal bone projection.	Nasal bone angle
Pn' to nTr	0.31	**0.80**	**0.76**	0.05	-0.27
Pn' to nCor	0.11	0.19	-0.24	**0.69**	-0.07
Sn' to nTr	0.24	**0.86**	**0.71**	0.18	-0.20
Sn' to nCor	0.02	0.04	-0.31	**0.64**	-0.05
Al' to alLSa	-0.20	0.07	0.01	-0.20	-0.07
Al' to nTr	0.33	**0.81**	**0.64**	0.09	-0.26
Al' to nCor	-0.07	-0.13	-0.42	0.49	0.07

Significant correlations ($p < 0.05$*) are indicated in bold.*

Regression equations (Figs 3 and 4 in supplementary material) and the results of cross-validations for black and white South Africans are described in Tables 7 and 8. From these regression equations, the nasal height and the nasal bone length were found to be significant predictors of the pronasale, subnasale and alare positions, while the nasal bone projection appeared as a consistent predictor only for the subnasale position in black and white South Africans. In addition, the nasal bone projection was also a consistent predictor for the pronasale position in white South Africans. The MSE for the regression equations of black South Africans ranged between 1.75 and 2.43 mm, and for white South Africans between 1.24 and 2.77 mm. The cross-validated accuracies for regression equations of black South Africans ranged between 87% and 100%, and for white South Africans between 79% and 100%. A cross-validation was also performed by applying the regression models (black/ white South Africans) of one group to the other group (black/white South Africans). The regression equations of white South Africans applied to the black South African sample showed a MSE ranging between 2.27 and 5.70 mm and, between 1.89 and 8.31 mm when the black South Africans regression equations were applied to the white South African sample. The regressions equations of white South Africans applied to the black South African sample showed accuracies ranging between 70% and 89% and, between 70% and 91% when the black South Africans regression equations were applied to the white South African sample.

Table 7. Stepwise multiple regression equations for predicting nose position of the black South African sample.

	Black South Africans equation regression				Cross-validation			
					Black sample		White sample	
		SE	R^2	*P-value*	MSEP	Accuracy	MSEP	Accuracy
Pronasale	Pn to NaTr = -17.805+1.170*Nasal height	5.69	0.64	**0.00**	1.89	88%	2.55	82%
	Pn to NaCor = 30.403-0.290*Nasal bone length	5.37	0.02	**0.00**	2.17	97%	8.31	87%
Subnasale	Sn to NaTr = -5.208+1.140*Nasal height	0.11	0.64	**0.00**	1.83	87%	1.89	78%
	Sn to NaTr = 29.723+1.092*Nasal bone length	2.67	0.54	**0.00**	1.82	91%	4.02	89%
	Sn to NaTr = 1.270+0.795*Nasal height+0.531*Nasal bone length	0.13	0.71	**0.00**	1.75	80%	2.32	70%
	Sn to NaCor = 3.063+1.060*Nasal bone projection	0.22	0.28	**0.00**	2.43	100%	3.30	87%
Alare	Al to NaTr = -7.148+1.036*Nasal height	0.12	0.56	**0.00**	1.79	84%	2.11	78%
	Al to NaTr = 25.608+0.943*Nasal bone length	2.93	0.42	**0.00**	1.86	88%	4.16	83%
	Al to NaTr = -2.369+0.782*Nasal height+0.391*Nasal bone length	0.15	0.61	**0.00**	1.88	88%	2.41	83%

SEE, standard errors of the estimates; R^2*, coefficient of determination. Significant values (*$p < 0.05$*) are indicated in bold. Mean Squared Error (MSE) using leave-one-out cross-validation and the accuracies of the regression equations using k-folds cross-validation.*

Table 8. Stepwise multiple regression equations for predicting nose position of the white South African sample.

	White South Africans				Cross-validation			
					White sample		Black sample	
		SE	R^2	P-value	MSEP	Accuracy	MSEP	Accuracy
Pronasale	Pn to NaTr = -7.969+0.963*Nasal height	0.09	0.64	**0.00**	1.79	90%	2.36	81%
	Pn to NaTr = 22.859+1.004*Nasal bone length	2.09	0.58	**0.00**	1.80	86%	3.56	84%
	Pn to NaTr = -1.341+0.633*Nasal height+0.554*Nasal bone length	0.11	0.74	**0.00**	1.77	83%	2.27	82%
	Pn to NaCor = 19.616+1.085*Nasal bone projection	1.90	0.48	**0.00**	1.90	98%	4.95	92%
Subnasale	Sn to NaTr = 2.950+0.991*Nasal height	0.07	0.75	**0.00**	1.52	86%	2.44	80%
	Sn to NaTr = 37.287+0.891*Nasal bone length	2.16	0.51	**0.00**	1.78	92%	4.08	88%
	Sn to NaTr = 6.850+0.797*Nasal height+0.326*Nasal bone length	0.09	0.79	**0.00**	1.24	79%	2.54	70%
	Sn to NaCor = 5.055+1.050*Nasal bone projection	0.16	0.41	**0.00**	1.94	100%	5.70	91%
Alare	Al to NaTr = 1.974+0.876*Nasal height	0.08	0.66	**0.00**	1.53	82%	2.61	79%
	Al to NaTr = 32.924+0.757*Nasal bone length	2.23	0.41	**0.00**	2.77	89%	4.16	83%
	Al to NaTr = 4.779+0.737*Nasal height+0.234*Nasal bone length	0.10	0.68	**0.00**	1.95	88%	2.68	83%

SEE, standard errors of the estimates; R^2, coefficient of determination. Significant values ($p < 0.05$) are indicated in bold. Cross-validation testing, Mean Squared Error (MSE) using leave-one-out cross-validation and the accuracies of the regression equations using k-folds cross-validation.

Discussion

In the process of approximating the nose, factors such as age, sex and ancestry must be considered. The growth and development of the human craniofacial skeleton results from the interdependence of its different components, which are influenced by multifactorial processes involving hormonal, genetic and epigenetic factors; and external stimuli (soft-tissue growth, dental maturation and various biomechanical factors) [32-43].

In forensic anthropology, estimation of ancestry from unknown skeletal remains is important for the development of a biological profile [44]. Ousley and collaborators [45] demonstrated that the morphological variability among population groups is quantifiable and may be useful in providing a probable classification of an unknown person. Data on the nose are also relevant to South African forensic artists and forensic anthropologists, especially in profile view to enhance facial recognition.

From the findings in this study, nasal height and nasal bone length might play important roles in the prediction of the shape of the nose in the frontal view in South Africans. The extent of nasal bone projection, on the other hand, could prove useful for the shape of the South African nose on profile views. Therefore, the morphology of the nose based on the pronasale, subnasale and alare positions, can potentially be estimated in an unknown black or white South African skull from the measurements of the nasal height, nasal bone length and nasal bone projection.

Although the nasal height, nasal bone length and nasal bone projection were significant and reproducible predictors for some of the positions of pn', sn' and al' in South Africans, not all surface landmark positions correlated significantly with the related hard- tissues. It is interesting to note that the nasal width and the nasal bone angle did not show any correlations with the external surface of the nose in both South African groups, while for the Korean population, all positions of the surface landmarks on the nose showed statistically significant correlations with the nasal bone and nasal aperture structure [19]. The value of our findings in the prediction of the al' by regression equations in both groups are limited. Indeed, the prediction on the alare relied only on a single vertical height measurement (al' to nTr) and not on any of the antero-posterior and lateral measurements.

From the recent literature, distinct differences in mid-facial size and shape have already been observed among all South Africans groups [46-48]. Indeed, in several osteometric analyses, some discrete traits from the mid-face, such as nasal width, inter-orbital breadth, nasal bone structure and alveolar prognathism have been shown to have a significant relationship

with ancestry for South African groups [46-52]. Our findings confirm that a significant hard- and soft-tissue morphological difference exists between black and white South Africans. The variation in the skeletal predictors of the external shape of the nose noted between black and white South Africans and the results of the cross-validation testing, emphasize the need for population specific guidelines and highlight the importance of considering ancestry as a factor in the process of approximating the nose. Variation in nasal hard- and soft-tissue morphologies has been described in other populations as well [14]. For instance, a highly significant difference of hard- and soft-tissue nasal shapes between Chinese and Europeans exists. While the nasal complexes in Chinese are smoother and incorporated into the skull, the European nasal shapes are quite prominent [14]. The failure of consideration of ancestral variation when developing approximation approaches may impact the accuracy of the final facial reconstruction.

Dimensions of the nose are important in distinguishing male and female faces and are useful in establishing an accurate facial approximation of a missing person through craniofacial reconstruction [4]. Although distinct differences in mid-facial morphology (size and shape) between the sexes are shown in many research studies [14,19,46,48,53,54], this may be less pronounced in the black South African group because of lower levels of sexual dimorphism in the cranium [46,47]. More precisely, these researchers observed that black South African males had a greater tendency for "intermediate" or "wide" nasal width and inter-orbital breadth than black South African females. In this study, the statistical analysis of sex differences in each group has shown a more important sexual dimorphism in white South Africans than in the black South African sample. It is important to emphasize that the findings on sexual dimorphism may to some extent be impacted by the sex split in each sample (60 black (23 females and 37 males) and 60 white (28 females and 32 males)). The differences between sexes observed confirm that growth for males and females is different. At birth, a slight sexual dimorphism exists, but the major divergence does not occur until puberty. As the adolescent growth spurt occurs approximately two years earlier in females than in males a longer development in males is induced, creating a significant sexual dimorphism in many body measures and therefore variations in the dimensions of the nose are not unexpected [4,33,41].

Currently, forensic artists in South Africa follow specific guidelines of soft-tissue thicknesses based on North American cadaver studies. Studies based on cadavers are influenced by desiccation, secular trends and population specificity, and the combination of these factors may affect the accuracy and validity of facial approximations in South Africa. As in the study by Lee and collaborator [19], we specifically used CBCT scans from living patients since we intended to remove the limits generated by the use of dry skulls, cadavers and CT datasets as initial references, such as desiccation and supination effects. A further advantage of CBCT compared to CT includes higher spatial resolution (0.1 mm to 0.4 mm) and isotropic volumetric data for the accurate placement of 3D landmarks and planes as required for this study [18].

An attempt was made to enhance the reproducibility and therefore the precision of the measurements by incorporating interplane distances, using coordinate values in the correlation between hard- and soft-tissue dimensions. In addition, great care was taken in the 3D head orientation by using a reslicing process following the FH planes. The utilization of coordinate values allows us to overcome the limits generated by the utilization of 3D hand tools such as the 3D head orientation during measurements.

The methodology resulting from this preliminary study on a South African sample needs to be applied to different populations and compared more intensively with other methods before it could be considered robust. In this study, we selected young adults in order to exclude possible remodelling effects of the facial skeleton with the advancement of age. When planning future research, it would be interesting to include more individuals of different age classes with a distinction between the sexes in order to observe possible effects of these factors on the

approximation of the nose and their possible significant relationship with ancestry. The utilization of CBCT scans from living patients negated the effects of desiccation and supination and provided a higher spatial resolution for the placement of 3D landmarks. It is important to emphasize that the measurement error is probably underestimated because single scans were re-measured, without rescanning the same subject.

Conclusion

The morphology of the nose based on the pronasale, subnasale and alare positions was found to have the potential to be estimated in an unknown black and white South African skull. From the findings, black and white South Africans, had significantly different hard- and soft-tissue morphology inducing the need for specific regression equations for both South African groups.

This study provides a possible reliable and reproducible method using CBCT scans and illustrates the importance of considering factors such as sex and ancestry in the process of approximating the nose.

Acknowledgments

The authors would like to thank Dr. André Uys from the Oral and Dental Hospital, University of Pretoria, South Africa and Dr. Sarel Botha from the Life Groenkloof Hospital, Pretoria, South Africa, for providing the CBCT-data. We acknowledge the AESOP+ consortia coordinated by Prof. José Braga from the Computer-assisted Palaeoanthropology Team, UMR 5288 CNRS-Université Paul-Sabatier, 37, allées Jules-Guesde, 31000 Toulouse, and from the Evolutionary Studies Institute and School of Geosciences, University of the Witwatersrand, Johannesburg, South Africa, for the financial support. We also thank the three anonymous reviewers for their constructive comments.

References

1. V. Bruce, G.W. Humphreys, Recognizing objects and faces, Visual Cognition. (1994); Apr 1;1(2–3):141–80. http://www.tandfonline.com/doi/abs/10.1080/13506289408402299.
2. S.H. Jeng, H.Y.M. Liao, C.C. Han, M.Y. Chern, Y.T. Liu, Facial feature detection using geometrical face model: An efficient approach, Pattern Recognition. (1998); Mar 1;31(3):273–82. https://doi.org/10.1016/S0031-3203(97)00048-4.
3. W. Zhao, R. Chellappa, P.J. Phillips, A. Rosenfeld, Face Recognition: A Literature Survey, ACM Computing Survevs. (2003); Dec;35(4):399–458. https://doi.org/10.1145/954339.954342.
4. E.P. Chronicle, M.Y. Chan, C. Hawkings, K. Mason, K. Smethurst, K. Stallybrass, You can tell by the nose—Judging sex from an isolated facial feature, Perception. (1995); 24(8):969–73. https://doi.org/10.1068/p240969.
5. W. Krogman, M. Işcan M, The Human Skeleton in Forensic Medicine, Charles C. Thomas Springfield IL, 2nd edition, 1986.
6. M.M. Gerasimov, face finder, CRC Press N Y NY, 1971.
7. R. George, The Lateral Craniographic Method of Facial Reconstruction, Journal of Forensic Sciences, Vol.32, No.5. (1987); pp.1305-1330. https://doi.org/10.1520/JFS11181J. ISSN 0022-1198.
8. M. Prokopec, D.H. Ubelaker, Reconstructing the shape of the nose according to the skull, Forensic Science Communications. (2002); 4(1).

https://archives.fbi.gov/archives/about-us/lab/forensic-science communications/fsc/jan2002/prokopec.htm.
9. C.N. Stephan, M. Henneberg, W. Sampson, Predicting nose projection and pronasale position in facial approximation: a test of published methods and proposal of new guidelines, American Journal of Physical Anthropology. (2003);122(3):240–50. https://doi.org/10.1002/ajpa.10300.
10. C. Rynn, C.M. Wilkinson, Appraisal of traditional and recently proposed relationships between the hard and soft dimensions of the nose in profile, American Journal of Physical Anthropology. (2006); Jul 1;130(3):364–73. https://doi.org/10.1002/ajpa.20337.
11. T.W. Todd, A. Lindala, Thickness of the subcutaneous tissues in the living and the dead, American Journal of Anatomy. (1928);41(2):153–196. https://doi.org/10.1002/aja.1000410202.
12. G.A. Macho, An appraisal of plastic reconstruction of the external nose, Journal of Forensic Sciences. (1986);31(4):1391–403. https://doi.org/10.1002/aja.1000410202.
13. F.M. Tilotta, J.A. Glaunès, F.J. Richard, Y. Rozenholc, A local technique based on vectorized surfaces for craniofacial reconstruction, Forensic Science International. (2010);200(1):50–9. https://doi.org/10.1016/j.forsciint.2010.03.029.
14. S. Schlager, Soft-tissue reconstruction of the Human nose, Population differences and sexual dimorphism, Dissertation, Albert-Ludwigs-Université de Fribourg. (2013). http://d-nb.info/1120020522.
15. P. Guyomarc'h, B. Dutailly, J. Charton, F. Santos, P. Desbarats, H. Coqueugniot, Anthropological Facial Approximation in Three Dimensions (AFA3D): Computer-Assisted Estimation of the Facial Morphology Using Geometric Morphometrics, Journal of Forensic Sciences. (2014);59(6):1502–16. https://doi.org/10.1111/1556-4029.12547.
16. N. Iblher, E. Gladilin, B.G. Stark, Soft-tissue mobility of the lower face depending on positional changes and age: a three-dimensional morphometric surface analysis, Plastic and Reconstructive Surgery. (2013); 131:372–381. https://doi.org/10.1097/PRS.0b013e318278d67c.
17. F. Marin, K. Ben Mansour, F. Demeter, P. Frey, Displacement of facial soft tissues in upright versus supine positions, Computer Methods in Biomechanics and Biomedical Engineering, (2015). https://doi.org/10.1080/10255842.2015.1069590.
18. W. C. Scarfe and A. G. Farman, What is Cone-Beam CT and how does it work? The Dental Clinics of north America. (2008); 52 707–730. https://doi.org/10.1016/j.cden.2008.05.005.
19. K.M. Lee, W.J. Lee, J.H. Cho, H.S. Hwang, Three-dimensional prediction of the nose for facial reconstruction using cone-beam computed tomography, Forensic Science International. (2014); 236:194-e1. https://doi.org/10.1016/j.forsciint.2013.12.035.
20. *J. Shindelin, I. Arganda-Carreras, E. Frise. et al, Fiji: an open-source platform for biological-image analysis, Nature methods. (2012); 9(7):676-682, PMID 22743772.* https://doi.org/10.1038/nmeth.2019.
21. A. Fedorov, R. Beichel, J. Kalpathy-Cramer, J. Finet, J.C. Fillion-Robin, S. Pujol, C. Bauer, D. Jennings, F. Fennessy, M. Sonka, J. Buatti, S.R. Aylward, J.V. Miller, S. Pieper, R. Kikinis, 3D Slicer as an Image Computing Platform for the Quantitative Imaging Network, Magnetic Resonance Imaging. (2012); Nov;30(9):1323-41. PMID: 22770690. https://doi.org/10.1016/j.mri.2012.05.001.
22. C.F. Spoor, F.W. Zonneveld, G.A. Macho, Linear measurements of cortical bone and dental enamel by computed tomography: applications and problems, American Journal of Physical Anthropology. (1993);91(4):469–84. https://doi.org/10.1002/ajpa.1330910405.

23. J. Buikstra, D. Ubelaker, Standards for data collection from human skeletal remains: Proceedings of a seminar at the Field Museum of Natural History (Arkansas Archaeology Research Series 44). *Fayetteville Arkansas Archaeological Survey*. (1994).
24. J. Caple, C.N. Stephan, A standardized nomenclature for craniofacial and facial anthropometry. *International journal of legal medicine*. (2016); *130*(3), 863-879. https://doi.org/10.1007/s00414-015-1292-1
25. G. Dahlberg, Statistical methods for medical and biological students. Statistical Methods for Medical and Biological Students, 1940.
26. G. Bräuer, R.Knussman, Grundlagen der Osteometrie. In Anthropologie, Handbuch der vergleichen Biologie des Menschen, Knussman R & Martin R, eds. Stuttgart, New York: Fisher. (1988); pp129-159.
27. J.M. Bland, D.G. Altman, Comparing methods of measurement: why plotting difference against standard method is misleading, The lancet. (1995);346(8982):1085–7. https://doi.org/10.1016/S0140-6736(95)91748-9.
28. B.H. Mevik, H.R. Cederkvist, Mean squared error of prediction (MSEP) estimates for principal component regression (PCR) and partial least squares regression (PLSR). *Journal of Chemometrics*, (2004); *18*(9), 422-429. https://doi.org/10.1002/cem.887
29. P. Burman, A comparative study of ordinary crossvalidation, v-fold cross-validation and the repeated learning–testing methods. Biometrika. (1989);76: 503–514. https://doi.org/10.1093/biomet/76.3.503
30. R. Kohavi, A study of cross-validation and bootstrap for accuracy estimation and model selection, in *Ijcai*. (1995); Vol. 14, No. 2, pp. 1137-1145. https://pdfs.semanticscholar.org/0be0/d781305750b37acb35fa187febd8db67bfcc.pdf
31. R Core Team. R: a language and environment for statistical computing. Vienna, Austria: R Foundation for Statistical Computing, (2012). http://www.R-project.org.
32. M.L. Moss, R.W. Young, A functional approach to craniology, American Journal of Physical Anthropology. (1960);18(4):281–92. https://doi.org/10.1002/ajpa.1330180406.
33. D.H. Enlow, M.G. Hans, Essentials of facial growth. W.B. Saunders Company; (1996).
34. M.L. Moss, The functional matrix hypothesis revisited. 1, The role of mechanotransduction, American Journal of Orthodontics and Dentofacial Orthopedics. (1997);112(1):8–11. https://doi.org/10.1016/S0889-5406(97)70267-1.
35. M.L. Moss, The functional matrix hypothesis revisited. 2, The role of an osseous connected cellular network, American Journal of Orthodontics and Dentofacial Orthopedics. (1997);112(2):221–6. https://doi.org/10.1016/S0889-5406(97)70249-X.
36. M.L. Moss, The functional matrix hypothesis revisited. 3, The genomic thesis, American Journal of Orthodontics and Dentofacial Orthopedics. (1997);112(3):338–42. https://doi.org/10.1016/S0889-5406(97)70265-8.
37. M.L. Moss, The functional matrix hypothesis revisited. 4, The epigenetic antithesis and the resolving synthesis, American Journal of Orthodontics and Dentofacial Orthopedics. (1997);112(4):410–7. https://doi.org/10.1016/S0889-5406(97)70049-0.
38. D.E. Lieberman, B.M. McBratney, G. Krovitz, The evolution and development of cranial form in Homo sapiens, Proceeding of the National Academy of Sciences of the United States of America. (2002);99(3):1134–9. https://doi.org/10.1073/pnas.022440799.
39. C.P. Klingenberg, K. Mebus, J. Auffray, Developmental integration in a complex morphological structure: how distinct are the modules in the mouse mandible? Evolution & Development. (2003);5(5):522–31. https://doi.org/10.1046/j.1525-142X.2003.03057.x.

40. Y. Tomoyasu, T. Yamaguchi T, A. Tajima, T. Nakajima, I. Inoue, K. Maki, Further evidence for an association between mandibular height and the growth hormone receptor gene in a Japanese population, American Journal of Orthodontics and Dentofacial Orthopedics. (2009);136(4):536–41. https://doi.org/10.1016/j.ajodo.2007.10.054.
41. D. Lieberman, The evolution of the human head. Harvard University Press; (2011).
42. F. Gröning, M. Fagan, P. O'higgins, Comparing the distribution of strains with the distribution of bone tissue in a human mandible: a finite element study, The Anatomical Record. (2013);296(1):9–18. https://doi.org/10.1002/ar.22597.
43. W.R. Atchley, B.K. Hall, A model for development and evolution of complex morphological structures, Biological Reviews. (1991);66(2):101–57. https://doi.org/10.1111/j.1469-185X.1991.tb01138.x.
44. J.T. Hefner, Cranial Nonmetric Variation and Estimating Ancestry. Journal of Forensic Sciences. (2009); 54: 985–995. https://doi.org/10.1111/j.1556-4029.2009. 01118.x.
45. S. Ousley, R. Jantz, D. Freid, Understanding race and human variation: Why forensic anthropologists are good at identifying race, American Journal of Physical Anthropology. (2009); Feb 18;139(1):68–76. https://doi.org/10.1002/ajpa.21006.
46. E.N. L'Abbé, C. Van Rooyen, S.P. Nawrocki, P.J, Becker, An evaluation of non-metric cranial traits used to estimate ancestry in a South African sample, Forensic Science International. (2011);209(1):195-e1. https://doi.org/10.1016/j.forsciint.2011.04.002.
47. J.L. McDowell, E.N. L'Abbé, M.W. Kenyhercz, Nasal aperture shape evaluation between black and white South Africans, Forensic Science International. (2012);222(1):397-e1. https://doi.org/10.1016/j.forsciint.2012.06.007.
48. J.L. McDowell, M.W. Kenyhercz, E.N. L'Abbé, An evaluation of nasal bone and aperture shape among three South African populations, Forensic Science International. (2015); 252:189-e1. https://doi.org/10.1016/j.forsciint.2015.04.016.
49. M. Steyn, E.N. L'Abbé, J. Myburgh, Forensic Anthropology as Practiced in South Africa, Hand book Forensic Anthropol Archaeol. (2016).
50. M.Y. İşcan, M. Steyn, Craniometric determination of population affinity in South Africans, International Journal of Legal Medicine. (1999);112(2):91–7. http://dx.doi.org/10.1016/S1353-1131(99)90011-1.
51. H. De Villiers, The skull of the South African Negro: a biometrical and morphological study. Witwatersrand University Press. (1968).
52. M. Napoli, W. Birkby, G. Gill, S. Rhine, Skeletal attribution of race: methods for forensic anthropology. Skeletal Attribution of Race Methods Forensic Anthropology. (1990).
53. S. Schlager and A. Rüdell, Analysis of the human osseous nasal shape—population differences and sexual dimorphism. American Journal of Physical anthropology (2015); 157:571–581. https://doi.org/10.1002/ajpa.22749. 2015.
54. P. Guyomarc'h and J.Bruzek, Dimorphisme sexuel du crâne de sujets identifiés (Collection Olivier, MNHN, Paris) : évaluation par morphométrie géométrique. Bulletins et mémoires de la Société d'anthropologie de Paris (2010) ; volume 22, Issue 3–4, pp 216–229. https://doi.org/10.1007/s13219-010-0019-6. 2010.

Supplementary material

Table 1 Supplementary material. Normality of the sample and measurement errors (ME) in mm.

Measurements (mm)	Abbreviation	Shapiro-Wilk test		ME	
		P-value	W	Inter	Intra
Nasal width	alLSa to alRSa	0.90	0.99	0.41	0.40
Nasal height	nTr to nsTr	0.06	0.97	0.72	1.06
Nasal bone length	nTr to rhiTr	0.43	0.98	0.43	0.64
Nasal bone projection	nCor to rhiCor	0.17	0.98	0.32	0.33
Nasal bone angle (°)	Nasal bone angle	0.97	0.05	0.70	0.40
Alare width	al'LSa to al'RSa	0.16	0.98	1.14	0.56
Pronasale to Nasion Transverse plane	pn'Tr to nTr	0.04	0.97	0.47	0.97
Pronasale to Nasion Coronal plane	pn'Cor to nCor	0.08	0.98	0.61	0.60
Subnasale to Nasion Transverse plane	sn'Tr to nTr	0.04	0.97	0.68	1.30
Subnasale to Nasion Coronal plane	sn'Cor to nCor	0.00	0.95	0.95	1.56
Alare to Right Nasal Cavity Sagittal plane	al'LSa to alLSa	0.25	0.98	0.74	0.48
Alare to Nasion Transverse plane	al'LTr to nTr	0.05	0.97	0.52	1.01
Alare to Nasion Coronal plane	al'LCor to nCor	0.03	0.97	1.38	1.61

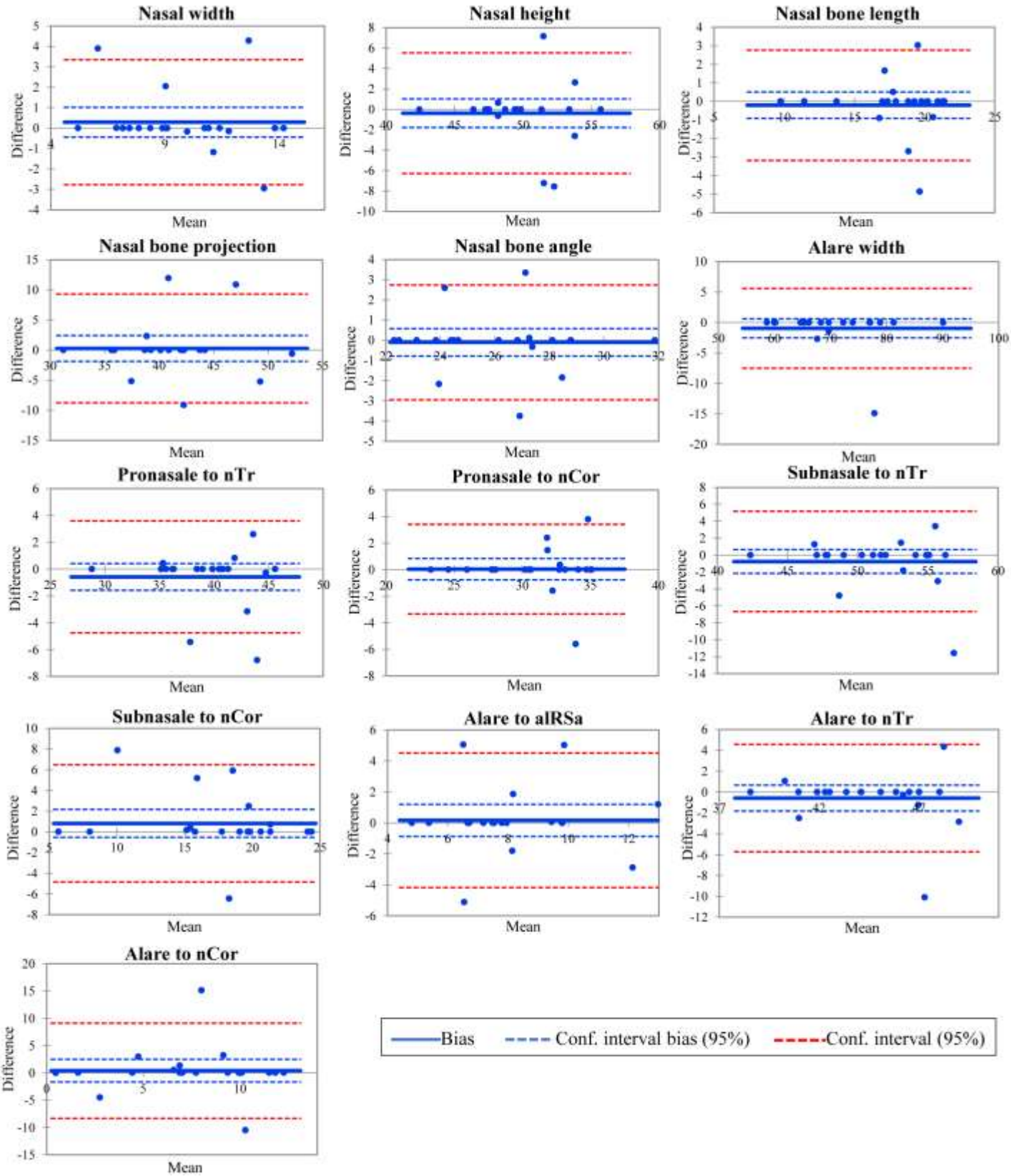

Figure 1 Supplementary material. Bland and Altman plots of the difference between inter-observer measurements. Mean (mm): (Observer1+Observer2)/2; Difference (mm): (Observer2-Observer1).

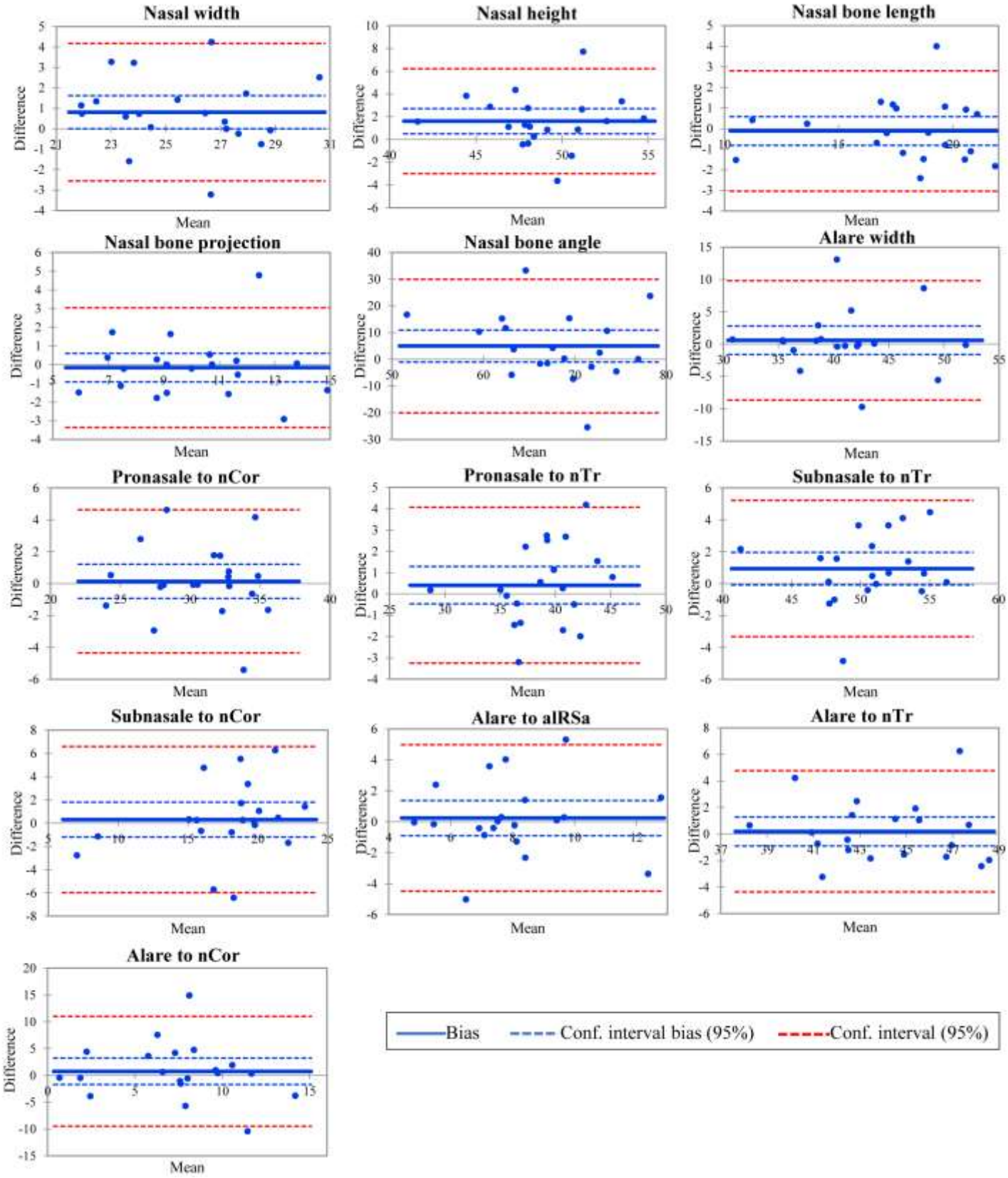

Figure 2. Supplementary material. Bland and Altman plots of the intra-observer errors. Mean (mm): (Observer1+Observer2)/2; Difference (mm): (Observer2-Observer1).

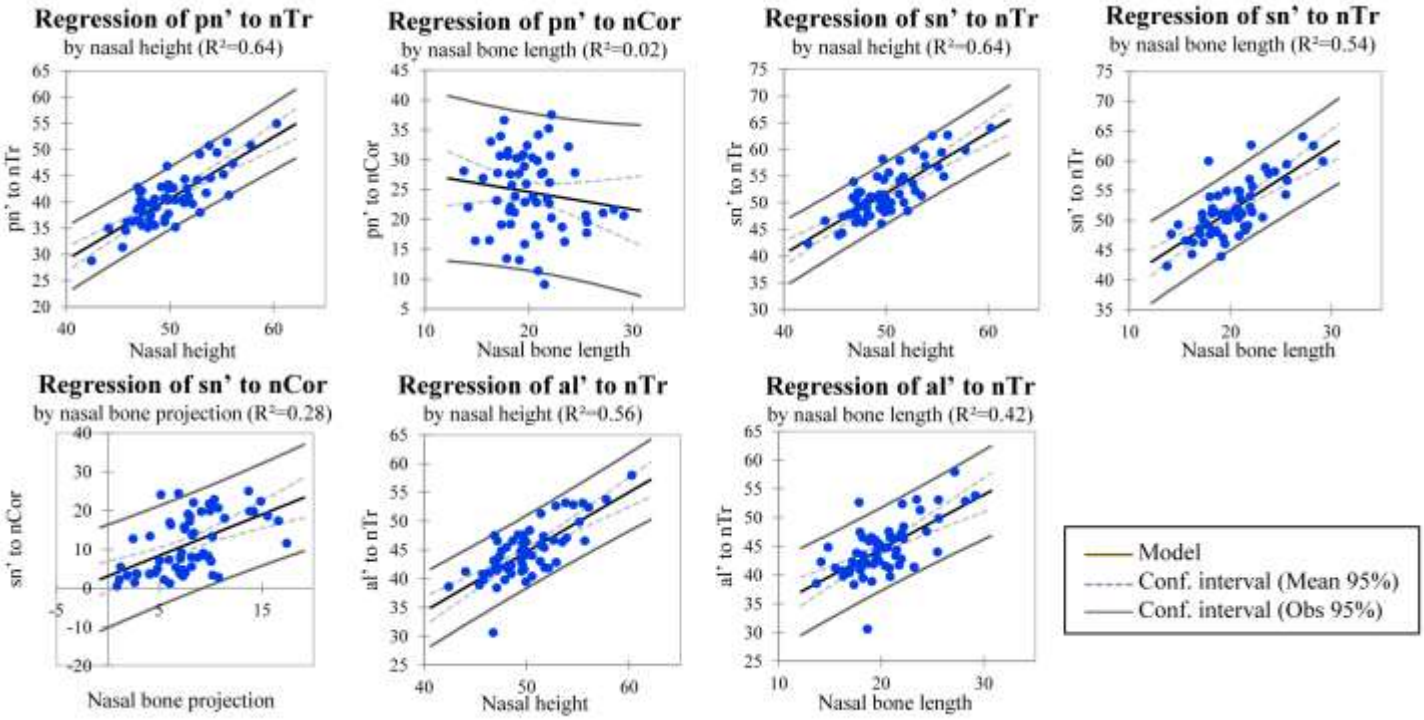

Figure 3. Supplementary material. Regression of pn', sn' and al' by nasal height, nasal bone length and nasal bone projection for the black South African population (cf. Table 7).

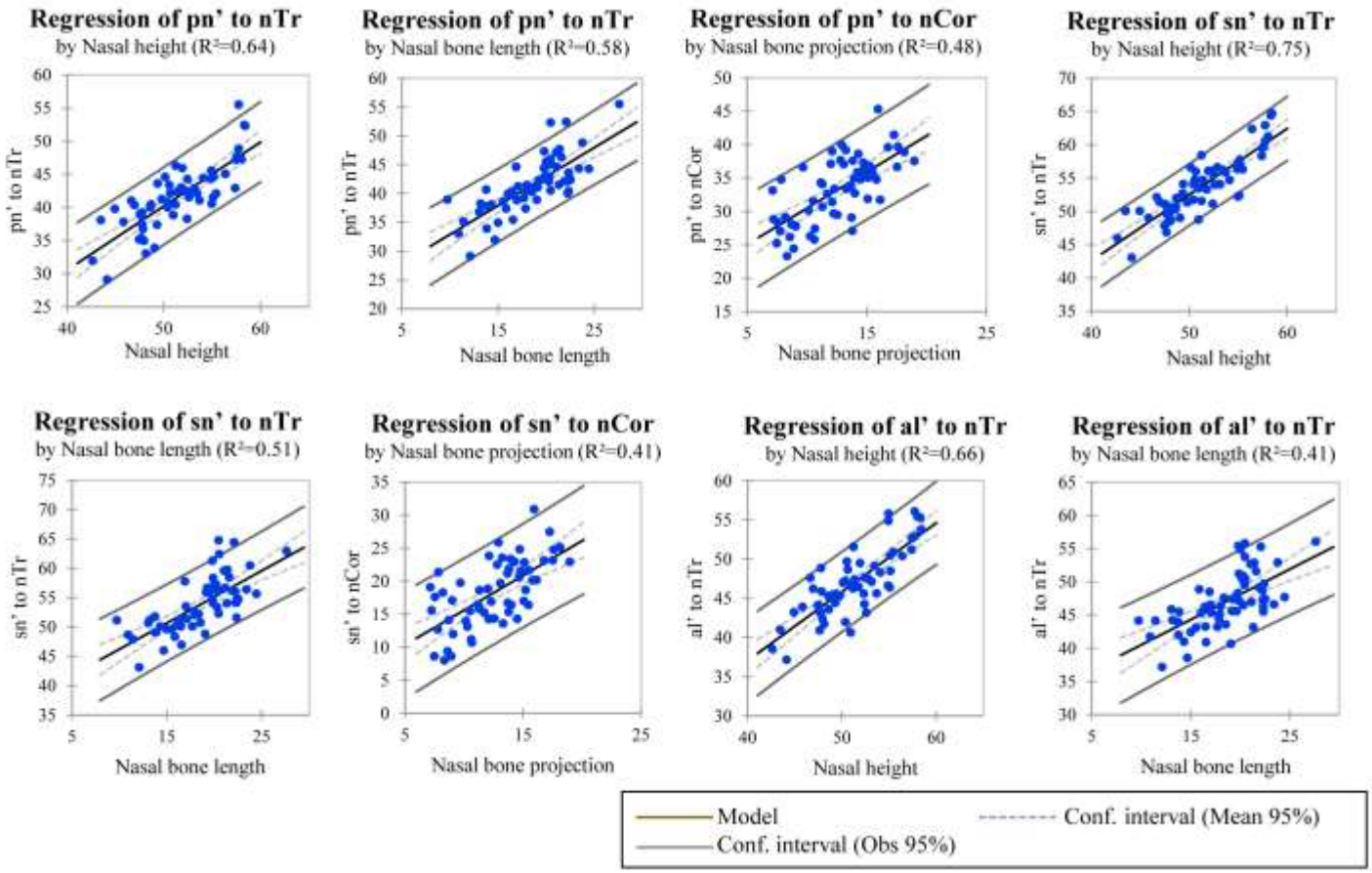

Figure 4. Supplementary material. Regression of pn', sn' and al' by nasal height, nasal bone length and nasal bone projection for the white South African population (cf. Table 8).